AN ANALYSIS OF NON-HOMOGENEOUS MATERIALS BY FRACTURE MECHANICS

Zhou Chengti (周承倜) Hu Yixiang (胡义祥)
Dalian Institute of Technology, China

Recently, many experiments show that S.G. cast iron holds many uncommon properties. Such as, its threshold value is higher and its transition temp. is lower than steel, and under that temp. it has higher impact toughness than steel[1-3]. We performed some micro-tension tests of S.G. cast iron and got: (1) the initial cracks always start from the internal central part of the specimen, and (2) the nucleation of the initial flaws often happen at the interface of bigger nodules, or at the boundaries of graphite flakes[4]. As to (1), we use the analytical solutions of elasticity for infinite medium. Because of (2), we take the central graphite nodule as a "main nodule", and solve a mixed boundary-value problem on the interface of main nodule. When considering the influence of the surrounding nodules, we suggest the stress function to be composed of two parts: one belongs to the main nodule and the other to the surrounding nodules. The latter is in random distributions, their average size and distance among them must be determined by the statistical method given by [5]. In [5] and [6], a stress function was contributed, the theoretical results were confirmed by the photoelastic tests[7], and from [7] we can conclude that to use the latter part of stress function to represent the influence of the surrounding nodules is valid. But in the work [4], the elastic property of nodules was neglected. We will show that the solution of such non-homogeneous materials is greatly influenced by the elastic property of the inclusions. We suppose two kinds of phase for inclusions: "soft-phase" and "hard-phase". For soft-phase: $\mu_0<\mu$, and for hard-phase: $\mu_0>\mu$. Here, μ_0 and μ are the shearing modulus of the inclusions and matrix, respectively. These two kinds of nodules bring out very different pictures of the stress and displacement fields, thus very different fracture phenomena. So it is important to consider the different elastic properties of inclusions for the non-

homogeneous materials.

I. STRESS FUNCTION AND ANALYTICAL SOLUTIONS

Stress function for the matrix (origin at the center of the main nodule, subscript j):

$$\Phi(z) = a_0 + \alpha_2(\frac{R_j}{z})^2 + \alpha_2(r_j)^2.C_{p1}(z)$$

$$\Psi(z) = b_0 + \beta_2(\frac{R_j}{z})^2 + \beta_4(\frac{R_j}{z})^4 + \beta_2(r_j)^2.C_{p1}(z) + \beta_4(r_j)^4.C_{p3}(z)$$

$$\phi(z) = \int\Phi(z)dz = a_0 z - \alpha_2(\frac{R_j^2}{z}) + \alpha_2(r_j)^2.D_1(z)$$

$$\psi(z) = \int\Psi(z)dz = b_0 z - \beta_2(\frac{R_j^2}{z}) - \beta_4(\frac{R_j^2}{3z^3}) + \beta_2(r_j^2).D_1(z) + \beta_4(r_j)^4.D_3(z)$$

here R_j is the radius of main nodule, R_s is the statistical average radius of surrounding nodules, the ratio $r_j = R_s/R_j$, and

$$C_{p1}(z) = \sum_{k=4,8,\ldots}^{\infty} C_k \gamma^k (\frac{z}{R_j})^{k-2}, \qquad C_{p3}(z) = \sum_{k=4,8,\ldots}^{\infty} C'_{k+4} \gamma^{k+4} (\frac{z}{R_j})^k$$

$$D_1(z) = \sum_{k=4,8,\ldots}^{\infty} C_k \gamma^k \cdot \frac{R_j}{k-1} (\frac{z}{R_j})^{k-1}, \qquad D_3(z) = \sum_{k=4,8,\ldots}^{\infty} C'_{k+4} \gamma^{k+4} \cdot \frac{R_j}{k+1} (\frac{z}{R_j})^{k+1}$$

where $\gamma = 4R_j/\xi$, ξ is the nearest distance between the centers of the main nodule and neighboring nodules. The values of C_k and C'_k are as follows:

$C_4 = -0.03696$, $C_8 = 0.4558\times10^{-3}$, $C_{12} = -0.2582\times10^{-5}$, $C_{16} = 0.14\times10^{-7}$, ...

$C'_8 = 0.2279\times10^{-2}$, $C'_{12} = -.3873\times10^{-4}$, $C'_{16} = .425\times10^{-6}$, $C'_{20} = -.35\times10^{-8}$, ...

Stress function for the main nodule (subscript o):

$$\Phi_0(z) = a_0\alpha'_0 + \sum_{k=2,4,\ldots}^{\infty} \alpha'_k (\frac{z}{R_j})^k, \quad \phi_0(z) = \int\Phi_0(z)dz$$

$$\Psi_0(z) = b_0\beta'_0 + \sum_{k=2,4,\ldots}^{\infty} \beta'_k (\frac{z}{R_j})^k, \quad \psi_0(z) = \int\Psi_0(z)dz$$

At the interface of the main nodule, $z=t=R_j e^{i\theta}$, the mixed boundary conditions are:

$$[\Phi(t)+\overline{\Phi(t)} + e^{2i\theta}(\bar{t}\Phi'(t)+\Psi(t))] = [\Phi_0(t)+\overline{\Phi_0(t)} + e^{2i\theta}(\bar{t}\Phi'_0(t) + \Psi_0(t))]$$

$$\frac{1}{2\mu}[\chi\phi(t) - t\overline{\phi'(t)} - \overline{\psi(t)}]e^{-i\theta} = \frac{1}{2\mu_0}[\chi_0\phi_0(t) - t\overline{\phi'_0(t)} - \overline{\psi_0(t)}]e^{-i\theta}$$

here χ and χ_0 are the functions of the Poisson's Ratio[7]. By solving the mixed boundary equations as above formalas, we can get complete solutions.

Stresses and displacements in matrix, $r \geq R_j$, are:

$$\sigma_r = \left\{2a_0 - \beta_2(\frac{R_j}{r})^2 + [4\alpha_2(\frac{R_j}{r})^2 - b_0 - \beta_4(\frac{R_j}{r})^4]\cos 2\theta\right\}$$

$$-\alpha_2(r_j)^2 \sum_{k=4,8,\ldots}^{\infty} kC_{k+4}\gamma^{k+4}(\frac{r}{R_j})^{k+2}\cos(k+2)\theta$$

$$-\beta_2(r_j)^2 \sum_{k=4,8,\ldots}^{\infty} C_k\gamma^k(\frac{r}{R_j})^{k-2}\cos k\theta - \beta_4(r_j)^4 \sum_{k=4,8,\ldots}^{\infty} C'_{k+4}\gamma^{K+4}(\frac{r}{R_j})^k\cos(k+2)\theta$$

$$\sigma_\theta = \left\{2a_0 + \beta_2(\frac{R_j}{r})^2 + [b_0 + \beta_4(\frac{R_j}{r})^4]\cos 2\theta\right\} + \alpha_2(r_j)^2 \sum_{k=4,8\ldots}^{\infty} KC_k\gamma^k(\frac{r}{R_j})^{k-2}\cos(k-2)\theta$$

$$+\beta_2(r_j)^2 \sum_{k=4,8,\ldots}^{\infty} C_k\gamma^k(\frac{r}{R_j})^{k-2}\cos k\theta + \beta_4(r_j)^4 \sum_{k=4,8,\ldots}^{\infty} C'_{k+4}\gamma^{k+4}(\frac{r}{R_j})^k\cos(k+2)\theta$$

$$\tau_{r\theta} = \left\{[2\alpha_2(\frac{R_j}{r})^2 + b_0 - \beta_4(\frac{R_j}{r})^4]\sin 2\theta\right\} + \alpha_2(r_j)^2 \sum_{k=4,8,\ldots}^{\infty} (k-2)C_k\gamma^k(\frac{r}{R_j})^{k-2}\sin(k-2)\theta$$

$$+\beta_2(r_j)^2 \sum_{k=4,8,\ldots}^{\infty} C_k\gamma^k(\frac{r}{R_j})^{k-2}\sin k\theta + \beta_4(r_j)^4 \sum_{k=4,8,\ldots}^{\infty} C'_{k+4}\gamma^{k+4}(\frac{r}{R_j})^k\sin(k+2)\theta$$

$$v_r = \frac{a_0 r}{2\mu}\left\{(\chi-1) + \frac{\beta_2}{a_0}(\frac{R_j}{r})^2 - [(\chi+1)\frac{\alpha_2}{a_0}(\frac{R_j}{r})^2 + \frac{b_0}{a_0} - \frac{\beta_4}{3a_0}(\frac{R_j}{r})^4]\cos 2\theta\right\}$$

$$+\left\{\alpha_2(r_j)^2 \sum_{k=4,8,\ldots}^{\infty} (\frac{\chi}{k-1} - 1)C_k\gamma^k r.(\frac{r}{R_j})^{k-2}\cos(k-2)\theta\right.$$

$$-\beta_2(r_j)^2 \sum_{k=4,8,\ldots}^{\infty} \frac{1}{k-1} C_k\gamma^k r(\frac{r}{R_j})^{k-2}\cos k\theta$$

$$\left.-\beta_4(r_j)^4 \sum_{k=4,8,\ldots}^{\infty} \frac{1}{k+1} C'_{k+4}\gamma^{k+4} r(\frac{r}{R_j})^k\cos(k+2)\theta\right\} \frac{1}{2\mu}$$

$$v_\theta = \frac{1}{2\mu}\left\{[\chi-1)\alpha_2 . r(\frac{R_j}{r})^2\sin 2\theta + b_0 r\sin 2\theta + \frac{\beta_4}{3} r(\frac{R_j}{r})^4\sin 2\theta]\right.$$

$$+\alpha_2(r_j)^2 \sum_{k=4,8,\ldots}^{\infty} (\frac{\chi}{k-1} + 1)C_k\gamma^k r(\frac{r}{R_j})^{k-2}\sin(k-2)\theta$$

$$+\beta_2(r_j)^2\sum_{k=4,8,..}^{\infty}\frac{1}{k-1}C_k\gamma^k.r(\frac{r}{R_j})^{k-2}\sin k\theta$$

$$+\beta_4(r_j)^4\sum_{k=4,8,..}^{\infty}\frac{1}{k+1}C'_{k+4}\gamma^{k+4}r(\frac{r}{R_j})^k\sin(k+2)\theta\Big\}$$

Stresses and displacements in main nodule, $r\leq R_j$, are:

$$\sigma_r^0=[2a_0\alpha'_0-\sum_{k=2,4,..}^{\infty}K\alpha'_{k+2}(\frac{r}{R_j})^{k+2}\cos(k+2)\theta]-[b_0\beta'_0\cos 2\theta$$
$$+\sum_{k=2,4,..}^{\infty}\beta'_k(\frac{r}{R_j})^k\cos(k+2)\theta]$$

$$\sigma_\theta^0=[2a_0\alpha'_0+\sum_{k=2,4,..}^{\infty}(k+2)\alpha'_k(\frac{r}{R_j})^k\cos k\theta]+[b_0\beta'_0\cos 2\theta$$
$$+\sum_{k=2,4,..}^{\infty}\beta'_k(\frac{r}{R_j})^k\cos(k+2)\theta]$$

$$\tau_{r\theta}^0=[2\alpha'_2(\frac{r}{R_j})^2+b_0\beta'_0]\sin 2\theta+\sum_{k=2,4,..}^{\infty}[(k+2)\alpha'_{k+2}(\frac{r}{R_j})^{k+2}+\beta'_k(\frac{r}{R_j})^k]\sin(k+2)\theta$$

$$v_r^0=\frac{1}{2\mu_0}\Big\{[\chi_0-1)a_0\alpha'_0r+\sum_{k=2,4,..}^{\infty}(\frac{\chi_0}{k+1}-1)\alpha'_kr(\frac{r}{R_j})^k\cos k\theta]-[b_0\beta'_0r\cos 2\theta$$
$$+\sum_{k=2,4,..}^{\infty}\beta'_k\frac{r}{(k+1)}(\frac{r}{R_j})^k\cos(k+2)\theta]\Big\}$$

$$v_\theta^0=\frac{1}{2\mu_0}\Big\{\sum_{k=2,4,..}^{\infty}(\frac{\chi_0}{k+1}+1)\alpha'_k.r(\frac{r}{R_j})^k\sin k\theta+b_0\beta'_0r\sin 2\theta$$
$$+\sum_{k=2,4,..}^{\infty}\beta'_k\frac{1}{k+1}r(\frac{r}{R_j})^k\sin(k+2)\theta\Big\}$$

When the surrounding nodules are far away from the main nodule, their influence upon the main nodule vanishes; in this case, the solution will degenerate to the exact solution of single inclusion[8].

For numerical computation, we take the carbon percentage C_w=3.4% in S.G. cast iron, then according to the statistical method [5], get ξ/R_j=4.7364. The numerical results are listed in Table 1.

II. CONCLUSIONS

(1) From Talbe 1, for soft-phase, the max. stress σ_θ at the interface of the bigger nodule (r_j<1), is greater than that of the smaller nodule (r_j>1), thus explains the observation (2).

(2) The SCF for multi-nodules (r_j>0) is always lower than single nodule case (r_j=0). This explains the threshold value of S.G. cast iron higher than steel.

(3) The endurance limit is in inversely proportional to SCF stress concentration factor. The theoretical curves computed by this paper are in agreement with the test data (Fig. 1).

(4) Biaxial effect is an important factor in fracture analysis[9]. Our results show that for soft-phase, under biaxial loading condition, all the above conclusions still hold.

(5) For hard-phase, the existence of many inclusions will greatly decrease SCF on the interface, and the stress distribution is much more uniform. In such case, max. stress σ_r happens at 0° on the interface, from this, we can calculate the seperation condition of the matrix and the main nodule. The solutions can also be used to compute the stress and displacement fields of dispersion (or particulate) hardening composite materials.

(6) On the interface, stresses σ_θ and σ_θ^0 are discontinuous, and the value of jumping stresses can easily be calculated by the formulas here.

REFERENCES

[1] Hu Yixiang, Estimates of the properties of S.G. cast iron by fracture mechanics, Nat. Conf. of Phys-chem. Analysis, Xamen, China, Nov. (1979).

[2] Owadano, T., Motoki, K., Tanigawa, E. and Kishitake, K., Fatigue crack propagation in S.G. cast iron, IMONO, Vol. 54, No. 5 May (1982) 284–288.

[3] Jolley,G. and Holdsworth,S.R., Ductile fracture initiation and propagation in ferritic S.G. cast iron, "Fracture", Vol. 2, ICF4 (1977).

[4] Zhou Chengti,Hu Yixiang, A Study of crack nucleation and propagation in nodular cast iron during tensile test, tech. paper of DIT (1982).

[5] Zhou Chengti and Hu Yixiang, An analysis of S.G. cast iron by fracture mechanics, 2nd Nat. Conf. of Fracture, Wuhang, China, (1980).

[6] Zhou Chengti, Analysis of the stresses in an elastic plane weakened by infinite rows of circular holes, Transacts of DIT, No. 1 (1960).

[7] Guan Changwen, Stress analysis of an elastic plane with many circular holes, Dissertation of M.D., Dept. of Engng. Mech., DIT, Oct. (1980).

[8] Muskhelishvili, N.I., Some basic problems of the mathematical theory of elasticity, 4th ed., Izd-vo AN SSSR (1954).

[9] Zhou Chengti, Kuo Chaopu, An Analysis of the mixed-type stress field near a crack-tip region, Engng. Fract. Mech., Vol. 16, No. 2 (1982) 35–47.

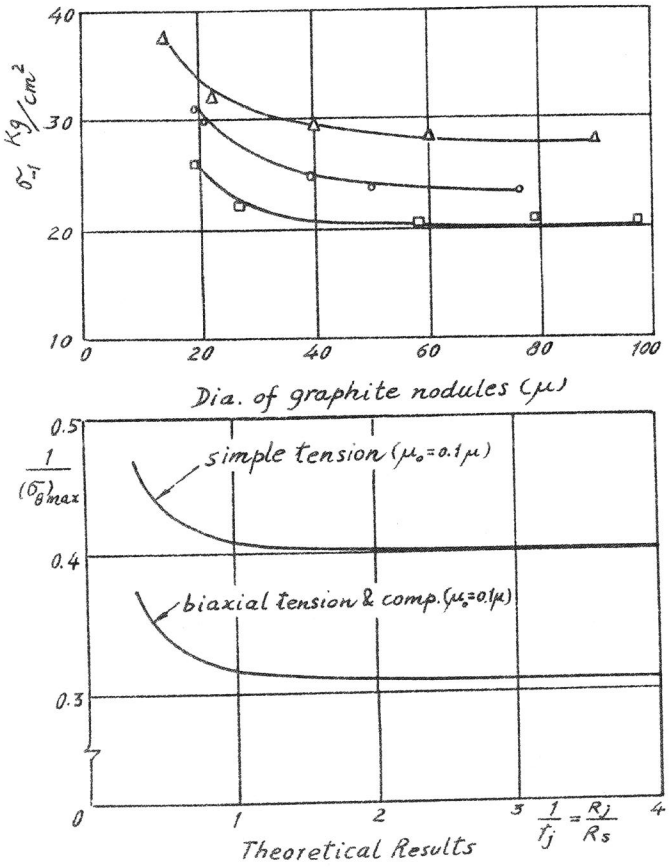

Fig. 1

Table 1

Stresses at the interface of the main nodule

simple tension		μ_0=0.1μ				μ_0=0.5μ				μ_0=1.5μ				μ_0=2.0μ			
$r_j=R_s/R_j$	θ	σ_r	σ_θ	σ_θ°	$\tau_{r\theta}$	σ_r	σ_θ	σ_θ°	$\tau_{r\theta}$	σ_r	σ_θ	σ_θ°	$\tau_{r\theta}$	σ_r	σ_θ	σ_θ°	$\tau_{r\theta}$
r_j=0	0°	0.25	-0.75	0	0	0.75	-0.25	-0.25	0	1.125	0.125	-0.455	0	1.2	0.2	-0.475	0
	45°	0.125	0.875	0.125	-0.125	0.375	0.625	0.125	-0.375	0.563	0.438	0.125	-0.563	0.6	0.4	0.125	-0.6
	90°	0	2.5	0.250	0	0	1.5	0.5	0	0	0.75	0.705	0	0	0.6	0.725	0
r_j=0.5	0°	0.252	-0.741	0.002	0	0.7506	-0.248	-0.249	0	1.125	0.124	-0.438	0	1.199	0.199	-0.477	0
	45°	0.123	0.877	0.127	-0.123	0.374	0.626	0.126	-0.374	0.563	0.437	0.125	-0.563	0.601	0.399	0.124	-0.601
	90°	0.002	2.488	0.245	0	0.001	1.497	0.498	0	-0.0003	0.751	0.689	0	-0.0004	0.602	0.728	0
r_j=1.0	0°	0.250	-0.717	0.009	0	0.7525	-0.242	-0.245	0	1.124	0.122	-0.442	0	1.198	0.196	-0.482	0
	45°	0.118	0.882	0.132	-0.116	0.373	0.627	0.127	-0.565	0.564	0.436	0.124	-0.565	0.602	0.398	0.123	-0.605
	90°	0.006	2.453	0.227	0	0.002	1.487	0.490	0	-0.001	0.755	0.694	0	-0.001	0.608	0.736	0
r_j=2.0	0°	0.291	-0.628	0.014	0	0.763	-0.220	-0.233	0	1.118	0.115	-0.452	0	1.189	0.185	-0.501	0
	45°	0.097	0.903	0.160	-0.085	0.366	0.635	0.135	-0.321	0.567	0.433	0.120	-0.575	0.608	0.392	0.117	—
	90°	0.015	2.322	0.166	0	0.006	1.451	0.465	0	-0.003	0.770	0.712	0	-0.004	0.630	0.766	0
r_j=3.0	0°	0.367	-0.517	0.016	0	0.788	-0.192	-0.223	0	1.105	0.106	-0.466	0	1.166	0.174	-0.527	0
	45°	0.006	0.939	0.189	-0.011	0.354	0.646	0.146	-0.596	0.573	0.427	0.114	-0.596	0.617	0.383	0.108	—
	90°	0.009	2.141	0.108	0	0.004	1.400	0.431	0	-0.001	0.7896	0.737	0	-0.0004	0.659	0.811	0